4.4A PRELIMINARY ANALYSIS OF THE VAISALA TLS200 NETWORK DEPLOYED DURING THE CHUVA CAMPAIGN IN BRAZIL

Martin J. Murphy*, Amitabh Nag, Jean-Yves Lojou, and Ryan K. Said
Vaisala Inc., Louisville, Colorado, U.S.

ABSTRACT:
As part of the CHUVA campaign in and around Sao Paulo, Brazil, in January - March 2012, Vaisala installed and operated a network of five of its new TLS-200 sensors. Each sensor includes both an LF component that measures the arrival times and angles and a VHF interferometer component that measures the arrival angles of VHF emissions primarily from cloud discharges. In this report, we present a preliminary analysis of the detection capability of the TLS-200 network, with a focus on cloud discharge detection and classification.

1. Introduction

From late October, 2011, to late March, 2012, the CHUVA campaign (Cloud processes of tHe main precipitation systems in Brazil: A contribUtion to cloud resolVing modeling and to the GPM (GlobAl Precipitation Measurement) was carried out in and around Sao Paulo, Brazil. As discussed by Albrecht et al (this conference), the primary objective of the campaign was to provide detailed information about the major types of precipitation systems that affect the region. In addition, total lightning observations were made by several different systems, and these were designed to be used as proxy data sets for upcoming geostationary lightning mapping instruments.

As part of CHUVA, Vaisala deployed a five-sensor network of its new TLS200 sensor. The TLS200 is the newest generation of the combined sensor having a VHF interferometer to determine the angles of arrival of emissions from cloud lightning discharges and an LF system that determines the angles and times of arrival of low-frequency emissions from cloud discharges as well as cloud-to-ground (CG) return strokes.

Cloud lightning detection performance is inherently difficult to quantify, but attempts to do so are quite valuable to end users trying to understand what a particular lightning detection system can provide. Cloud lightning detection at LF, where fewer sensors can be used to cover a given area, is considered to have growing importance. Given this, our objective is to quantify the cloud lightning detection capabilities of the TLS200 network deployed in CHUVA, particularly flash detection efficiency (DE) but also spatial mapping capability. This analysis was carried out using a number of small thunderstorms with discrete flashes on 16 January 2012.

*Corresponding author address: Martin J. Murphy, Vaisala Inc., 194 S. Taylor Ave., Louisville, CO 80027 U.S.; e-mail: martin.murphy@vaisala.com

2. Lightning detection systems

The five-sensor TLS200 network is shown in Figure 1. The distances between neighboring sensors ranged from 55 to 130 km, and the longest distance across the network was 160 km.

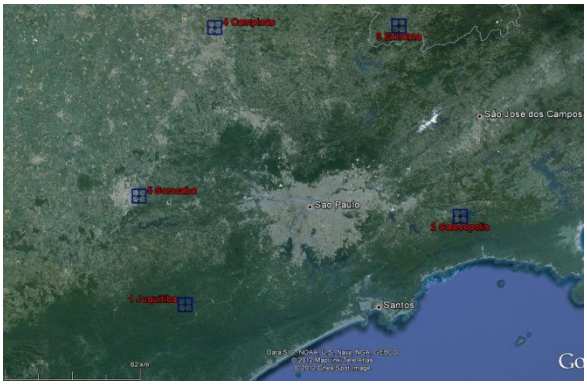

Figure 1. Google Earth image showing the five Vaisala TLS200 sensors deployed during the CHUVA campaign.

The reference lightning network during the CHUVA campaign was a 12-sensor Lightning Mapping Array (LMA; Thomas et al. 2004) deployed closer to the city of Sao Paulo itself. The LMA has been demonstrated to detect cloud flashes and the in-cloud and leader components of CG flashes with nearly 100% DE. The LMA typically geolocates individual VHF emission sources within discharges with a spatial accuracy on the order of 100 meters or better.

3. Data set and analysis methods

Unlike CG lightning, where high-speed video and tower measurements can readily be used to count discrete return strokes and flashes, cloud

lightning activity can be difficult to assess quantitatively because of the optical obstruction of the cloud, the often extensive horizontal channel structure, and the high rate of cloud discharge activity in many thunderstorms. Primarily for the latter reason, we wanted to identify some periods of low flash-rate storms with discrete flashes that could fairly readily be counted by hand if necessary. Some of the lightning activity on 16 January 2012 satisfied these criteria, so we chose to analyze a subset of the storms on this date.

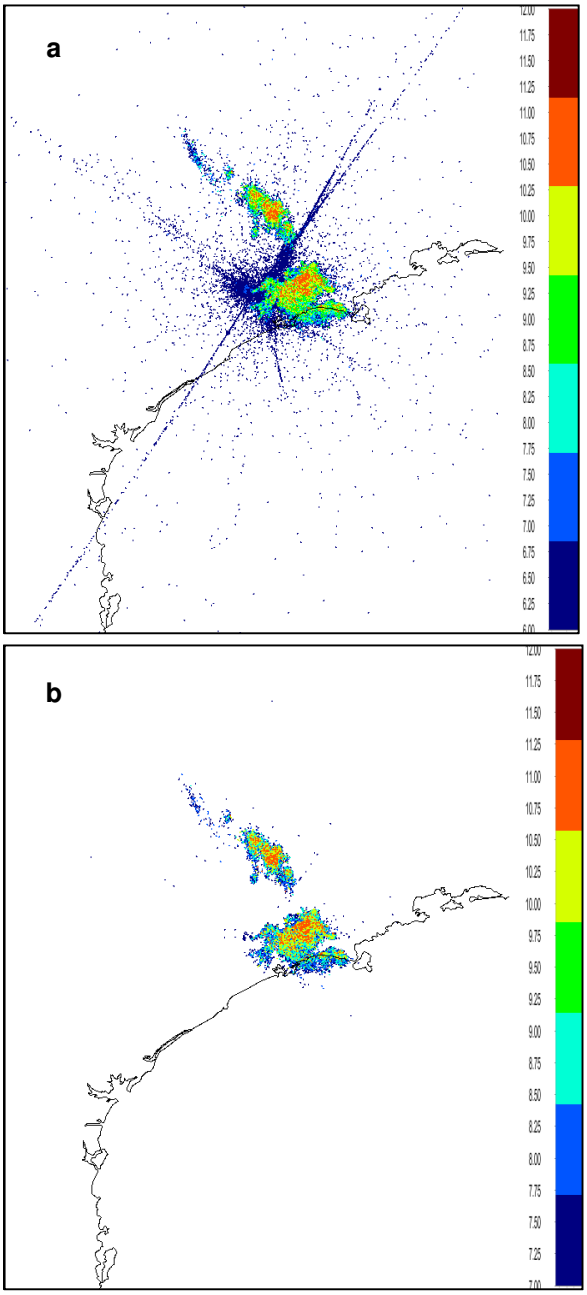

Figure 2. (a) original LMA data from 00:00 – 01:00 UTC on 16 January; (b) after removal of all sources detected by only 6 sensors.

The original, raw LMA data from 00:00-01:00 UTC on 16 January are shown in Figure 2a. The color scale shows the number of contributing stations from 6 to 12. In addition to thunderstorms, a lot of noise and several long streaks are also seen in the data. These were totally dominated by events with only 6 contributing sensors. To start the analysis, we therefore removed all 6-sensor detections from the LMA data set. This resulted in a significantly cleaner data set, shown in Figure 2b. On further examination, however, we also found a number of sources at low altitudes that occurred on a quasi-continuous basis. Figure 3 shows an altitude-time plot from the first 10 minutes of the day, together with LF data from the TLS200 network. Discrete lightning flashes are clearly visible in the sources above about 3.5 km altitude, but below that, numerous sources are also seen. While these tend to be more concentrated around lightning flashes, they are also spread throughout the time period. Our second step in processing the data was to remove all sources with altitudes below 3.5 km.

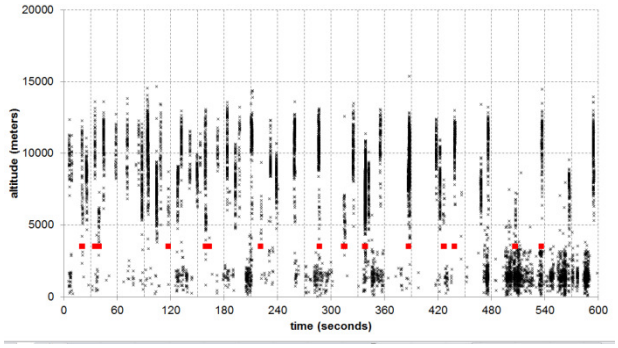

Figure 3. Altitude-time plot of LMA (small black x) between 00:00 – 00:10 UTC on 16 January. LF events from the TLS200 network are shown as small red squares. The LF events have no altitude; they are simply plotted at 3500 for ease of viewing.

The VHF sources from the TLS200 network are shown in Figure 4, together with two regions that were specifically chosen because of the low-rate lightning activity. The color scale in Fig. 4 is time of day in 24 steps. In the larger, southern box, the maximum total flash rate observed by the TLS200 was 51 flashes in five minutes and

occurred at 17:20 UTC. In the smaller, northern box, the maximum was 60 flashes in five minutes at 20:45 UTC. At most times, both regions exhibited total flash rates of 30 or fewer per five minutes. Each region contained a couple of thunderstorm cells between 00-03 UTC (dark colors) and a few scattered cells from 16:00 UTC onward (yellow to red).

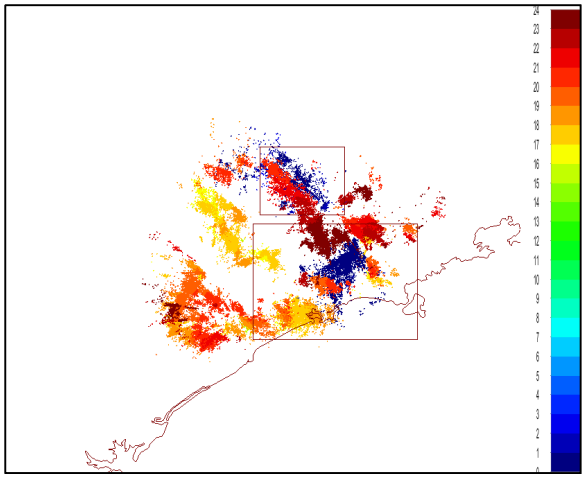

Figure 4. VHF sources from the TLS200 network color-coded by time of day (UTC) in 24 steps. The boxes show the regions of isolated, low flash rate storms that were analyzed in this study.

Although total flash rates were generally low enough to permit manual counts, to insure uniform flash counting, we employed the source grouping algorithm described by Lojou and Cummins (2005). This algorithm forms branches, and ultimately flashes, from individual VHF sources by connecting the sources that are closest together given some maximum space and time constraints. As discussed by Murphy (2006), however, this source grouping algorithm (and others) is susceptible to producing excessive flash counts especially as either the time or distance constraint is lowered. To make sure that the default values of these constraints were appropriate to both TLS200 and LMA flash data sets, we undertook a sensitivity analysis over the first hour of 16 January. Table 1 summarizes the results from the TLS200 analysis in the southern box from Figure 4. The default constraint values (12 km and 500 msec) are in the center of the table. The typical sensitivity to both time and distance constraints is observed here. In the case of LMA (not shown), greater sensitivity to the distance constraint than the time constraint was observed in this data set because we explicitly removed LMA flashes with only one or two sources. The default grouping constraints led to a total of 163 flashes from the TLS200 and 164 from LMA, and both were consistent with a manual count of 161. Thus, we concluded that it was appropriate to use the default time and distance constraints to group the VHF sources into flashes.

Table 1. Sensitivity of TLS200 VHF flash count over the first hour of 16 January to the time and distance contraints of the grouping algorithm. To facilitate viewing, the distance constraint values in km on the left side of the table are highlighted in orange, and the time constraint values in msec along the top are highlighted in yellow. All flash counts within 10% of 163, the value obtained with the default constraints, are highlighted in green.

	time constraint (msec)							
km	200	300	400	500	600	700	800	900
2	1335	1249	1209	1184	1177	1174	1173	1173
4	614	554	528	521	515	514	512	512
6	354	323	302	296	290	290	290	290
8	265	231	219	212	208	208	208	208
10	224	194	182	176	173	173	173	173
12	211	182	169	163	161	161	161	161
14	193	163	152	147	145	145	145	145
16	189	157	146	139	136	136	136	136
18	186	154	144	137	134	134	134	134
20	185	152	142	134	131	130	130	130

To match flashes from the VHF systems with the LF data from the TLS200 network, we determined the minimum and maximum latitude and longitude bounds containing the VHF sources from each flash and then added a 10-km buffer around that to search for matching LF events. Additionally, matching LF events were required to fall within the time bounds defined by the first and last VHF sources in the flash with a small time buffer. That time buffer was set to 100 msec with LMA data. In the TLS200 sensors, the VHF component of the TLS200 was set to limit its bandwidth consumption by transmitting no more than 333 events per second. This could result in the partial cut-off of flashes that would otherwise have been detected fully, and thus, we raised the time buffer to 250 msec when matching TLS200 VHF flashes to LF data. A sensitivity test over a larger data set showed that an additional 5 to 7.5% of VHF flashes could end up having matched LF events if either the time or

space buffers were increased to as large a 1 second and 50 km, but then, some unrealistic matches would certainly be included. Thus, we decided to leave the space and time buffers as described here.

We began by matching CG strokes from the LF part of the TLS200 network to VHF flashes. Those VHF flashes that matched were set aside into a "known CG" flash set, and the remaining VHF flashes were assumed to be cloud flashes and set aside as the "known IC" set. Then, we matched all cloud discharges detected by the LF part of the TLS200 network to the "known CG" and "known IC" flash sets. Naturally, the in-cloud and leader components associated with CG flashes could be detectable by the LF portion of the TLS200 network, so we wanted to investigate whether the LF part of the network gave equal, worse, or better performance when detecting cloud discharge components associated with CG flashes. This was the motivation behind separating the two flash sets. The "total lightning" detection efficiency of the LF cloud discharge data set was then easily determined by recombining the results from the separate flash sets.

4. Results

Tables 2a and 2b respectively summarize the counts of flashes in the "known IC", "known CG" and total sets and the cloud discharge detection efficiency of the LF part of the TLS200 network with respect to each set.

From table 2a, we note that the southern box from Figure 4 exhibits more consistency in flash counts between the LMA and TLS200 than the northern box, particularly in the "known IC" set. We have not undertaken a thorough investigation of why the TLS200 flash counts are notably higher in the northern region, but it is reasonable to suggest that either (1) our filtering of the LMA data may have removed too much from that area, and/or (2) location accuracy issues may have pulled more TLS200 VHF data into the northern region from areas farther out.

In table 2b, we see that the LF part of the network systematically detected cloud discharge activity in a higher percentage of CG flashes than cloud flashes. In the southern box, the CG flash detection efficiency was in the mid-60% range, while the known IC flash DE was either 47% or 54% depending on whether the LMA or TLS200 was the source of the VHF flash information. A wider discrepancy was noted in the northern box, where CG flash DE was either 84% or 74% depending on VHF data source, but the known IC flash DE was either 40% or 49%. The total lightning flash DE was generally in the low 50% range. Previous verification of total flash DE was presented by Murphy et al. (2006) using a set of test sensors embedded within the U.S. NLDN with sensor separations similar to those in the CHUVA project. That analysis showed total flash DE values between 17 and 38%. The higher values now observed with the TLS200 are a promising sign of substantially improved LF cloud discharge detection.

Table 2a. Counts of flashes in the "known IC", "known CG", and total flash sets from both VHF networks in the southern and northern boxes from Figure 4.

	southern box		northern box	
	LMA	TLS200	LMA	TLS200
known IC	1097	1089	720	795
known CG	418	502	126	181
total	1515	1591	846	976

Table 2b. Detection efficiencies, in percent, based on cloud discharges detected by the LF component of the TLS200 network, with respect to the "known IC", "known CG", and total flash sets from both VHF networks in the southern and northern boxes from Figure 4.

	southern box		northern box	
	LMA	TLS200	LMA	TLS200
known IC	47.3	54.5	48.8	39.6
known CG	68.7	66.5	84.1	74.0
total	53.2	58.3	54.0	46.0

In prior Vaisala LF networks with limited cloud lightning detection capability, it was nominally assumed that at most one cloud discharge would be detected per flash. The above-mentioned analysis by Murphy et al. (2006), however, did take into account the possibility of more than one per flash, but again, that involved an embedded network with shorter sensor separations. In this study, having demonstrated that the TLS200 network exhibits significantly better overall cloud lightning performance, we turn to the number of cloud discharge events detected by the LF part of the system per flash. Figure 5 shows the results from the southern box using the LMA

known IC flash set, from which the LF cloud flash DE of the TLS200 system was found to be 47.3% (Table 2b). Of the 519 LMA known IC flashes that had matching cloud discharge events from the TLS200 LF system, only 36% (189 flashes) had just a single LF cloud discharge, while 13% (67 flashes) had at least five LF cloud discharges, and one flash had 11.

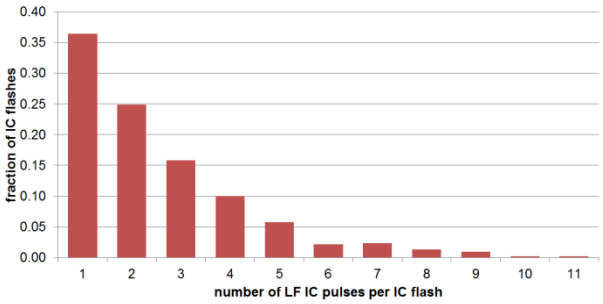

Figure 5. Number of LF cloud discharge pulses detected per known IC flash from the LMA set over the southern box from Figure 4.

Figures 6a and 6b show two examples of large cloud flashes that were detected multiple times by the LF component of the TLS200 network. In each figure, the colors indicate time, with the flash broken down into 10 (Fig. 6a) or 9 (Fig. 6b) equal-time segments. The small dots show the LMA points, while the larger squares show the LF cloud discharges detected by the TLS200 system.

The flash in Fig. 6a occurred at 18:24:49 and had 241 LMA points and eight LF cloud discharge detections. All eight LF events were detected within the first 40 msec of the flash, whose total duration was 370 msec. Seven of the eight LF discharge positions appear to be well located insofar as their positions are within the area where LMA detected VHF sources during the same 40 msec.

The second sample, Fig. 6b, occurred at 17:35:42, had a total duration of 620 msec, 290 LMA sources, and seven LF cloud discharge events. In this example, the seven LF events were spread over 337 msec and covered much more of the spatial extent of the flash than in the case of Fig. 6a. In fact, one LF event was detected near the northernmost end of the flash at the same time that the LMA showed VHF sources in the same area. Another LF event that occurred about 164 msec earlier was fortuitously

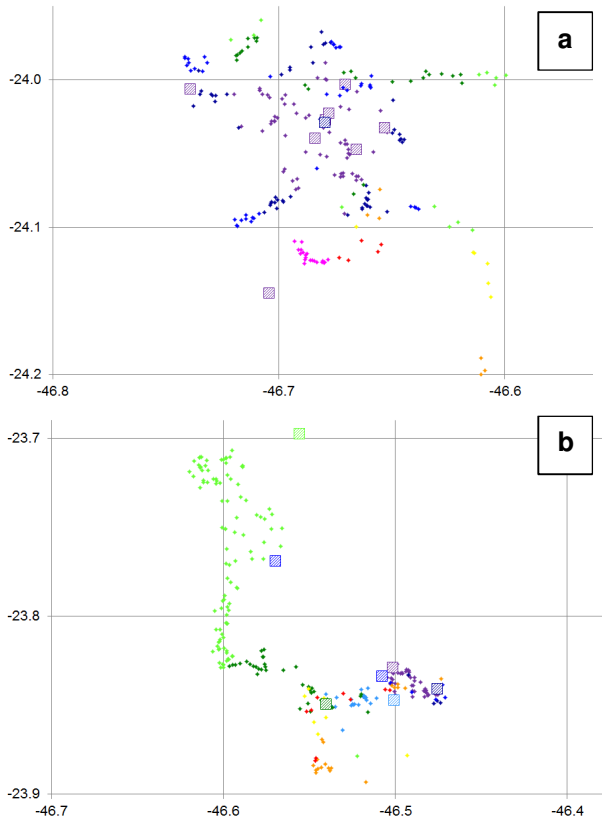

Figure 6. Two cloud flashes having multiple detections by the LF part of the TLS200 network. Small dots are LMA sources, and larger squares are LF events. The horizontal and vertical axes are longitude and latitude, respectively. Colors represent time over the duration of each flash. (a) 18:24:29 UTC; (b) 17:35:42 UTC/

located near that same northern channel but not at the correct time. It actually appears to have been associated with earlier activity that occurred closer to the flash origin.

5. Conclusions and future work

In this study, we have used small thunderstorms with low total lightning rates to document the LF cloud discharge detection performance of the Vaisala TLS200 system deployed during the CHUVA project. The LF part of the system consistently detected about 50% of all lightning flashes in these storms, whether the LMA or the VHF part of the TLS200 system was used as the total lightning reference. We also found that the LF system was able to detect multiple cloud discharges in more than half the flashes that it detected, and most of the positions of these discharges were consistent with the LMA data.

In early 2013, Vaisala is rolling out enhancements to both the TLS200 sensor and the central processor software to improve both sensitivity to, and geolocation of, cloud discharges by the LF component of the sensors. These enhancements were not in place at the time of the CHUVA campaign, so the results presented above represent a baseline level of performance that is expected to improve further. For example, the position inaccuracies in the LF cloud discharges shown in Figs. 6a and 6b could easily be associated with inaccurate pulse time alignment when different sensors detect different members of a train of LF pulses associated with a single cloud discharge event. The combination of sensor and central processor improvements in the upcoming release includes the means to address pulse trains and the proper time alignment of pulses.

6. References

Albrecht, R.I., et al., 2013: CHUVA lightning mapping field campaigns: First results and contributions to GOES-R and MTG, this conference, paper TJ30.3.

Lojou and Cummins 2005 On the representation of two- and three-dimensional total lightning information. Proceedings, First Conference on the Meteorological Applications of Lightning Data, San Diego, CA, U.S., Amer. Meteorol. Soc.

Murphy, M.J., 2006: When flash algorithms go bad. Proceedings, 1st International Lightning Meteorology Conf., Tucson, AZ, U.S., Vaisala, Inc.

Murphy, M.J., Demetriades, N.W.S., Holle, R.L., and Cummins, K.L., 2006: Overview of capabilities and performance of the U.S. National Lightning Detection Network. Proceedings, 2nd Conf. on Meteorological Applications of Lightning Data, Atlanta, GA, U.S., Amer. Meteorol. Soc.

Thomas, R.J., Krehbiel, P.R., Rison, W., Hunyady, S.J., Winn, W.P, Hamlin, T., Harlin, J., 2004: Accuracy of the Lightning Mapping Array. *J. Geophys. Res.*, **109**, doi: 10.1029/2004JD004549